Trajectory Control Strategy Applied to Autonomous Vehicles

Barbara Pinheiro Santo André
Lucas Martins Morello
Gustavo Yukio Yamazaki
Gabriel Kazuo Izumi
Luiz Adalberto Barboza Júnior
Fabrício Leonardo Silva
Felix M. Escalante
Institute of Science and Technology of Sorocaba - São Paulo State University - UNESP, Sorocaba, Brazil

ABSTRACT

Autonomous vehicles represent a major technological advancement in the transportation sector, with the potential to significantly reshape urban mobility. Ensuring their safe and efficient operation demands control systems that are secure, precise, and adaptable, i.e., capable of responding in real time to dynamic environmental conditions while planning and adjusting trajectories in accordance with the vehicle's physical constraints. Within this framework, trajectory control plays a fundamental role in enabling the vehicle to follow a predefined path with high precision. This paper proposes the development of a trajectory control strategy for a 1:10 scale autonomous vehicle. The control strategy will be derived from a mathematical model that accurately represents the vehicle's dynamic behavior. To assess the performance of the proposed system, the vehicle will be tested through simulations involving various trajectories, including complex paths and scenarios with changing environmental conditions. These simulations will evaluate the system's ability to maintain trajectory accuracy and adaptiveness, thereby validating its potential for real-world applications.

INTRODUCTION

In recent decades, there has been significant progress in the development of autonomous vehicles, with applications ranging from civilian transportation and goods delivery to robotics. These systems operate in diverse and dynamic environments, requiring robust control strategies to ensure safe and efficient navigation (1). Among the classical trajectory control approaches, the Pure Pursuit method stands out due to its simplicity and satisfactory performance in smooth trajectories. This algorithm operates based on the idea of "pursuing" a target point ahead of the vehicle, which is recalculated in real time according to the geometry of the desired trajectory and the presence of obstacles in the environment (2; 3; 4).

In this work, we investigate the application of the Pure Pursuit algorithm in the context of a 1:10 scale autonomous electric vehicle, taking into account the specific characteristics of the control system, vehicle dynamics, and the constraints imposed by the simulated environment. This analysis allows us to assess the effectiveness of the method in controlled scenarios, serving as a foundation for future applications in more complex vehicular systems.

In addition to the steering control techniques presented in Table 1, several approaches have been proposed in the literature for autonomous vehicle control, either through the introduction of new strategies or by optimizing existing methods—often combining them with other complementary techniques, such as the control types presented in (3). In this work, the Pure Pursuit algorithm was chosen as the main steering control strategy due to the use of a controlled and obstacle-free environment, which provides ideal conditions for its operation.

As discussed in (2; 3; 4), Pure Pursuit may present limitations in scenarios with obstacles or abrupt trajectory changes, such as the "shortcut" effect during curves. However, by restricting the vehicle's operation to moderate speeds and predefined paths, these limitations are significantly mitigated. Furthermore, Pure Pursuit offers high efficiency in curves, requires only a few trajectory points to estimate curvature, and is easy to implement—resulting in low computational cost. For these reasons, it remains one of the most widely used classical approaches in autonomous vehicle control, particularly in prototyping and testing applications in simplified environments.

BLDC motors (Brushless Direct Current) are widely used in vehicle propulsion systems due to their superior characteristics compared to conventional motors. Their structure mainly consists of two elements: the stator, which is the stationary part responsible for generating a variable magnetic field through three-phase coils, and the rotor, which contains

Table 1. Types of Steering Control

Control Strategy	Reference	Application
Pure Pursuit	Harshit and Priyal (2)	Controlled environments and moderate-speed scenarios
PID	Yang and Liu (5)	Low-speed models and improved stability
LQR	Zheng et al. (1)	High-speed scenarios with good maneuverability
Fuzzy	Rasib et al. (3)	Complex and nonlinear models

permanent magnets and rotates in response to the generated magnetic field (6).

The operation is based on the sequential electronic commutation of the stator phases, where each coil alternately receives voltages of different levels (high, medium, and low) (7), creating a rotating magnetic field that drives the rotor. As a result of this configuration, BLDC motors offer significant advantages such as higher torque density, high efficiency, compact size, low maintenance cost, and quiet operation. These features make BLDC motors particularly suitable for small autonomous electric vehicle applications, such as the one used in this work (6).

For the proper operation of BLDC motors, the use of an ESC (Electronic Speed Controller) is essential. The ESC is responsible for controlling the speed and direction of rotation of the motor. It performs the electronic commutation of the motor's three phases, sequentially activating each of the stator coils with different voltage levels (high, medium, and low). This sequence generates a rotating magnetic field that interacts with the permanent magnets on the rotor, driving its rotation in the desired direction (6).

Therefore, the main objective of this article is the development of an autonomous vehicle aimed at competitions, integrating multiple areas of knowledge such as computer vision, control, electronics, and mechanics. The central focus is the implementation of a steering control strategy based on the Pure Pursuit algorithm, aiming to ensure precise and stable vehicle navigation in controlled environments.

LONGITUDINAL DYNAMIC

The analysis of the forces acting on a vehicle during straight-line motion is known as longitudinal dynamics. In this work, the main forces that significantly affect the dynamic behavior of a 1:10 scale vehicle are considered. Among these, the following stand out: rolling resistance (R_x), aerodynamic drag (R_a), the weight component related to road slope ($W \sin\theta$), the drawbar pull force (R_{hx}), and the traction force provided by the propulsion system (F_x) (8).

By applying Newton's Second Law in the longitudinal direction, we obtain Eq. (1) (8):

$$\sum F_X = Ma_x = F_x - R_x - R_a - W\sin(\theta) - R_{hx} \quad (1)$$

Considering the characteristics of the competition — small-scale vehicle, no towed load, and simulations carried out on a flat track — the effects of road slope and drawbar pull force can be neglected, that is, $W\sin(\theta) = R_{hx} = 0$. Thus, the longitudinal dynamic model is reduced to the analysis of traction force and rolling resistance.

A. Rolling Resistance

At low speeds, typically below 50 to 60 km/h, rolling resistance (R_x) is the predominant resistive force influencing the longitudinal motion of the vehicle (8). This resistance is associated with the deformation of the tires as they interact with the road surface, resulting in energy losses. Rolling resistance can be expressed by Eq. (2), as a function of the vehicle's weight (W), the road slope angle (θ), the vehicle speed in meters per second (V), and the rolling resistance coefficient (f_r), which is empirically determined as described in Eq. (3) (8).

$$R_x = f_r W \cos\theta \quad (2)$$

$$f_r = 0{,}01\left(1 + \frac{2{,}24V}{100}\right) \quad (3)$$

B. Aerodynamic Drag

Aerodynamic drag is related to the interaction between the vehicle and the surrounding airflow. Due to the complexity of the flow over the vehicle body, it is common to approximate the aerodynamic drag force (R_a) using Eq.(4), as described in (8). This resistance depends on the air density (ρ), the drag coefficient (C_d), the vehicle's frontal area (A_f), and the relative velocity between the vehicle and the air (V_R), as presented in Eq.(5) (8).

$$R_a = \frac{1}{2}\rho C_d A_f V_R^2 \quad (4)$$

The relative velocity V_R is determined by the vehicle's speed (V) added to or subtracted from the wind speed (V_{ar}), depending on the direction of the wind relative to the vehicle's movement:

$$V_R = V \pm V_{ar} \quad (5)$$

Given the physical characteristics of the vehicle under study, the magnitude of this force is small when compared to rolling resistance and the traction force.

C. Vehicle Transmission System

The vehicle's traction system consists of a BLDC motor, model 3670/4T, responsible for providing torque to the rear wheels. Power is transmitted from the motor to the rear axle through a reduction gearbox with a 1:10 ratio, directly coupled to the drive axle. For motor control, an ESC capable of handling a peak current of 80A, model B08HHCHFD2, was used to ensure appropriate response and speed control of the motor's rotation.

In the simulation of the vehicle's longitudinal behavior, a constant speed was considered. This simplification allowed for a reduction in model complexity and enabled the isolation of rolling resistance effects, providing a clearer analysis of this force's influence on the vehicle's performance under steady-state conditions.

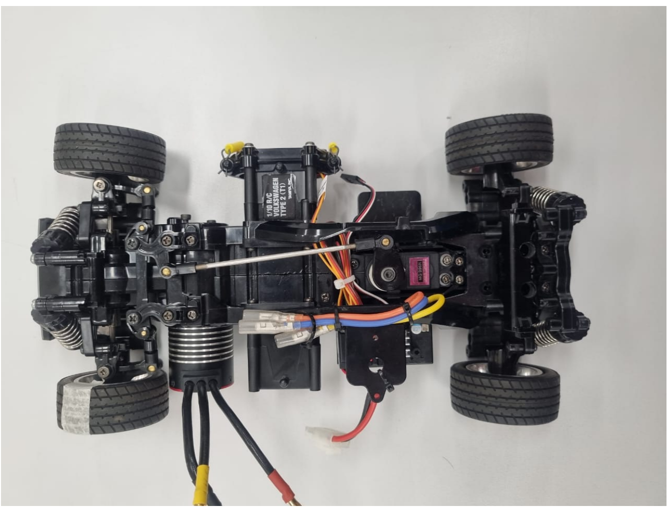

Figure 1. Scale vehicle used as the basis for dynamic simulations.

LATERAL DYNAMIC

Lateral dynamics studies the behavior of a vehicle during transverse movements, such as cornering and changes in direction, involving forces and motions perpendicular to the trajectory. However, due to the small scale of the vehicle under study, this work opts to disregard the complex lateral forces acting during turns and focuses exclusively on analyzing the steering angle.

When making a turn, a vehicle's front wheels must be aligned according to the desired steering angle. During this maneuver, the steering angles of the front wheels differ from each other, as the inner wheel follows a trajectory with a smaller radius compared to the outer wheel, as illustrated in Fig. 2. One of the most commonly used approaches to model this behavior in low-speed turns is the Ackermann steering geometry.

To simplify the analysis of Ackermann geometry, it is common to represent the vehicle using the so-called **bicycle model** (8). In this model, the system is reduced to two wheels: one front and one rear, analogous to the configuration of a conventional bicycle, as shown in Fig. 3.

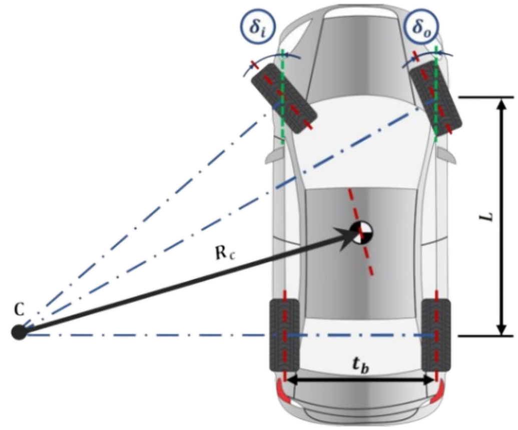

Figure 2. Illustration of a vehicle making a turn around the center of curvature C with radius R_c (8).

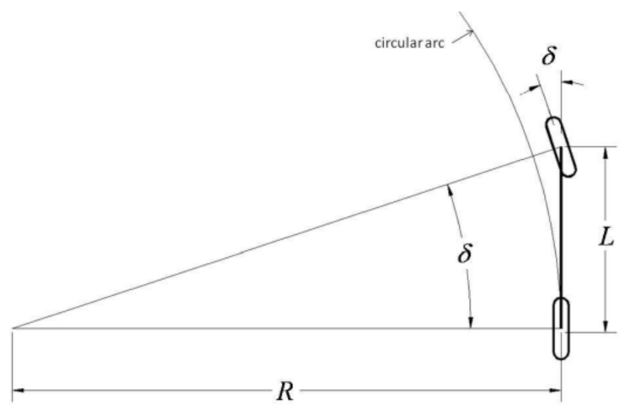

Figure 3. Representation of the bicycle model and the following parameters: steering angle (δ), the radius of the circle that the rear axle will follow under a given steering angle (R), and the distance between the front and rear wheels (L) (9).

Considering low speeds and moderate steering angles, the bicycle model allows the steering angle to be approximated using Eq. (6), as presented in (4):

$$\tan(\delta) = \frac{L}{R} \tag{6}$$

AUTONOMOUS VEHICLE CHARACTERISTICS

For the simulations, a small-scale vehicle was used, as illustrated in Fig. 1. The main physical parameters of the model are presented in Table 2.

Table 2. Physical parameters of the scaled vehicle.

Parameter	Value
Wheelbase L [m]	0.22
Track width [m]	0.15
Longitudinal distance from the center of mass to the front axle [m]	0.088
Longitudinal distance from the center of mass to the rear axle [m]	0.132
Vertical distance of the center of mass [m]	0.064
Total mass M [kg]	1.256
Yaw inertia [kg·m^2]	0.04
Frontal area [m^2]	0.02
Drag coefficient (C_d)	0.3

CONTROL STRATEGY

The Pure Pursuit method is a geometric approach for trajectory tracking in autonomous vehicles, in which the steering control is achieved by pursuing a point ahead of the vehicle, known as the lookahead point. This point is defined as a point (g_x, g_y) belonging to the desired trajectory, as shown in Fig. 4, located at a distance l_d, the lookahead distance, ahead of the vehicle's current position. The trajectory, in turn, is generated by an onboard vision system, which detects the track and provides the next three points of the path.

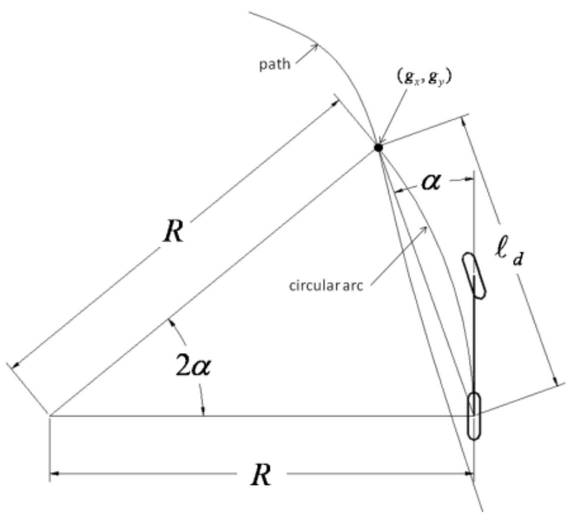

Figure 4. Geometric representation of Pure Pursuit in which a vehicle follows an arc-shaped trajectory with radius R and angle α (9).

Once the current position of the vehicle is determined, the next point on the trajectory is identified. This point then becomes the next lookahead point, and the line connecting the vehicle's position to the lookahead point defines the direction the vehicle will follow. The angle representing the difference between the vehicle's orientation and the line of sight to the lookahead point is then calculated. (4).

Based on this angle and the distance l_d, the radius of curvature that the vehicle should follow to smoothly reach the target point is determined, assuming that its trajectory follows a circular arc. By applying the Law of Sines in Fig.4, Eq.(7) is obtained:

$$\frac{\ell_d}{\sin(2\alpha)} = \frac{R}{\sin\left(\frac{\pi}{2} - \alpha\right)}$$

$$R = \frac{l_d}{2\sin(\alpha)} \tag{7}$$

Using Eqs.(6) and (7), the steering angle is obtained, which can be described by Eq.(8).

$$\delta = \tan^{-1}\left(\frac{2L\sin(\alpha)}{l_d}\right) \tag{8}$$

Where δ represents the steering angle, L is the distance between the front and rear axles of the vehicle, α is the angle between the vehicle's orientation and the line to the lookahead point, and l_d is the lookahead distance (4).

The value of δ is then converted into a control signal and transmitted to a motor responsible for the physical adjustment of the front wheel. This motor acts directly on the steering system, performing the turn corresponding to the arc that connects the vehicle to the lookahead point.

This process occurs continuously within a control loop. In each new cycle, the vision system updates the vehicle's position and the trajectory points. The steering angle is then recalculated and applied to the actuator. The loop remains active until the final destination is reached.

The flowchart in Fig. 5 illustrates the operation of the pure pursuit algorithm.

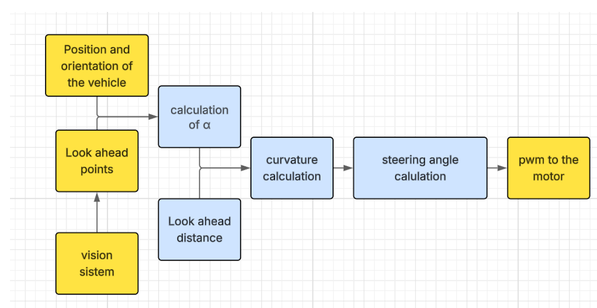

Figure 5. Flowchart of the Pure Pursuit algorithm.

RESULTS

The evaluation of the developed trajectory control strategy was carried out through simulations in two distinct scenarios: a single isolated curve and the complete circuit used in competitions. The data obtained were analyzed considering both the fidelity of the path followed relative to the reference trajectory and the behavior of the steering angle applied by the controller.

Fig.6 presents the simulation results for a simple curve. In Fig.6a, the vehicle's trajectory is represented by the continuous blue line, while the reference points, indicating the desired trajectory, are shown as red dots. It can be observed that the path followed by the vehicle closely tracks the reference line, demonstrating that the Pure Pursuit controller was able to guide the vehicle effectively, even in a scenario with a sharp curvature. Fig. 6b shows the steering angle signal of the vehicle. Upon analyzing its behavior, it is noted that the variation occurs in a discrete and less linear manner than initially expected. This characteristic may be related to the discretization of control commands or the sensitivity of the parameters used. Nevertheless, the overall system response is positive, as the trajectory remained stable and within expected limits, validating the application of the strategy for this type of maneuver.

Fig.7 shows the data obtained during the simulation of the complete circuit, representing a more complex environment with varied maneuvering requirements. Overall, the vehicle's trajectory remained close to the reference line throughout the entire path, demonstrating that the control system was able to handle the curvature and directional changes imposed by the track layout. However, the analysis of the steering signal reveals an irregular actuation pattern, with frequent oscillations between extreme values and zero. This characteristic suggests intermittent control behavior, possibly resulting from low command granularity or the absence of filtering in the output signal. Although such behavior did not compromise trajectory tracking in the simulation, it raises concerns regarding the practical application of the strategy in a physical vehicle, which would require a more continuous and smoother control response to preserve the stability and integrity of the steering system.

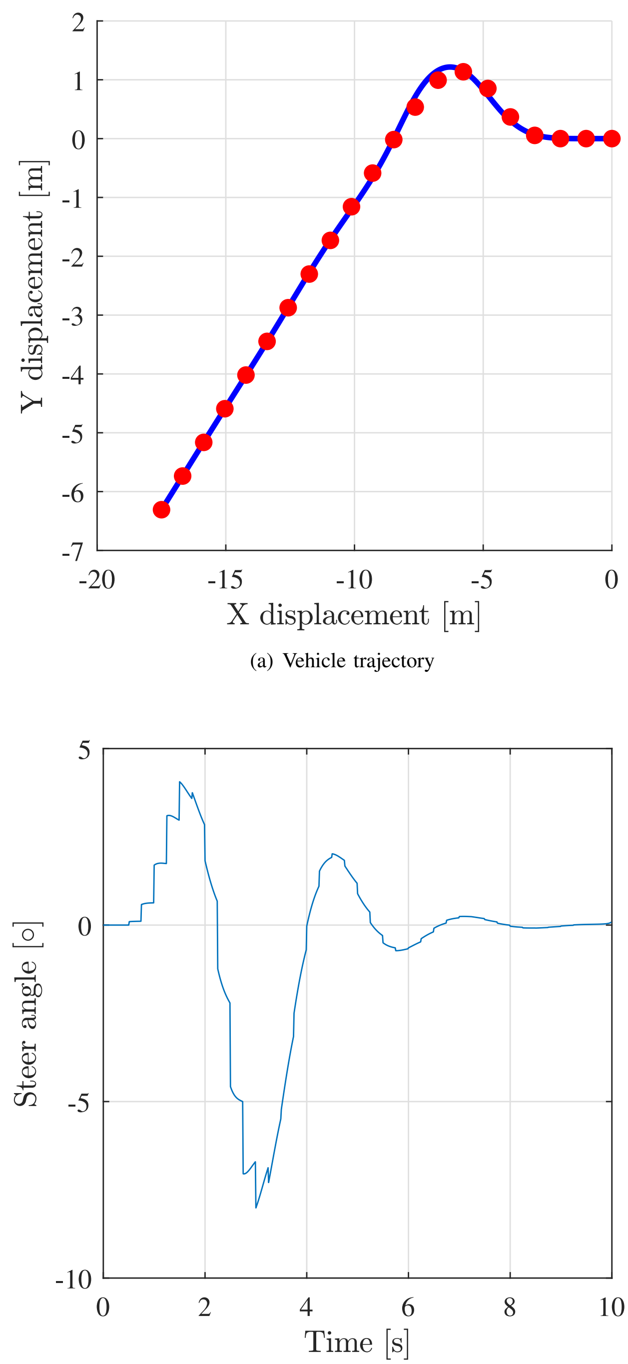

(a) Vehicle trajectory

(b) Steering angle

Figure 6. Simulation of a maneuver *sine wiht dwell*

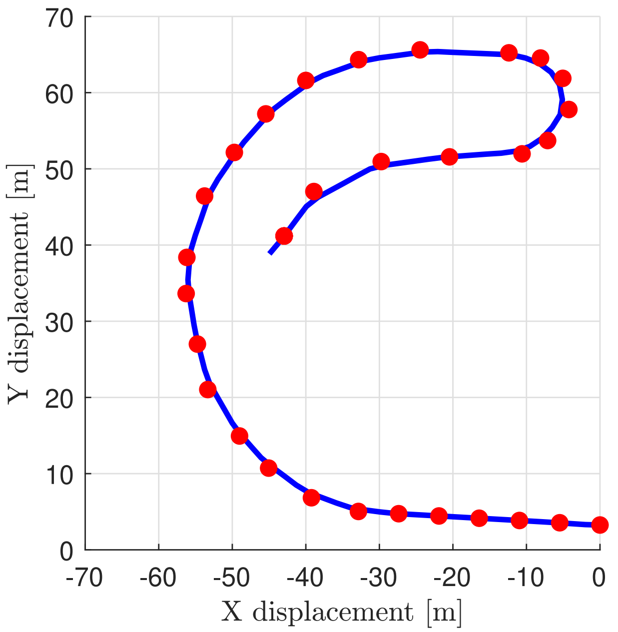

(a) Vehicle trajectory

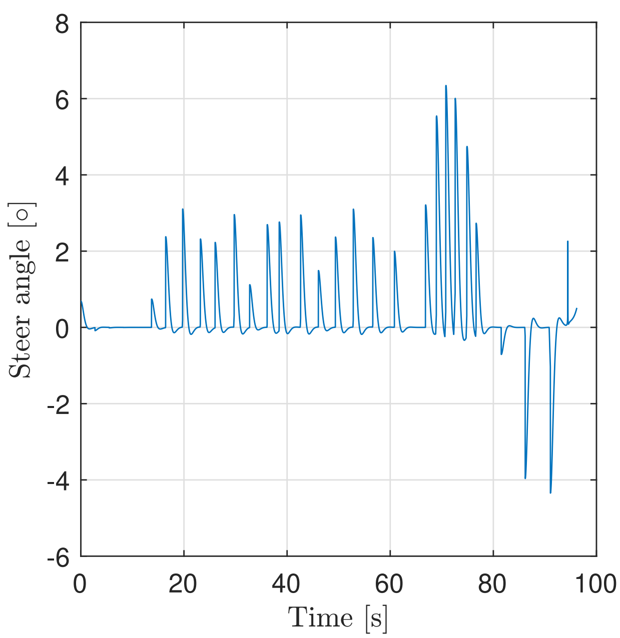

(b) Steering angle

Figure 7. Simulation of the competition circuit

CONCLUSION

The main objective of this work was the development and evaluation of a trajectory control strategy based on the Pure Pursuit algorithm, applied to a 1:10 scale autonomous vehicle, with a focus on competitions in controlled environments. From its conception, the proposed approach aimed to integrate aspects of vehicle dynamic modeling, embedded control implementation, and autonomous navigation through computer vision, establishing a trajectory tracking technique.

The results obtained through simulations demonstrated that the implemented strategy was effective in guiding the vehicle with high accuracy along predefined trajectories, including sharp turns. The path fidelity with respect to the reference line met the established performance criteria, indicating that the Pure Pursuit algorithm—even in its classical form—is suitable for applications in simplified and controlled environments, such as the simulated competition scenarios analyzed in this study.

However, the analysis of the steering angle behavior revealed important aspects to be considered in future work. It was observed that the control signal generated exhibits discrete variations and abrupt oscillations under certain conditions, indicating intermittent operation of the steering system. Although this behavior did not compromise the trajectory in the simulation, it may pose a risk to the stability and mechanical integrity of the vehicle in practical applications, where a smoother and more continuous steering actuator response is required.

Therefore, it is concluded that, although the control strategy achieved the fundamental goals of navigation and trajectory tracking, there is significant room for improvement, particularly with respect to refining the steering angle control. Future investigations may incorporate signal smoothing techniques, adaptive control, or fusion with other control methods in order to enhance the robustness and quality of real-time response. Moreover, practical validation through physical vehicle testing will be essential to confirm the feasibility of the proposed system and to guide the necessary adjustments for its implementation in real-world environments.

ACKNOWLEDGMENT

The authors would like to thank LUNAR (University League of Autonomous Navigation and Robotics) at the UNESP Sorocaba campus for their technical support and encouragement of research, as well as AEAS – Association of Engineers and Architects of Sorocaba, the league's sponsor, for their financial support in the development of this project. Special thanks are also extended to Professors Fabrício Leonardo Silva and Felix M. Escalante for their guidance and valuable contributions throughout the course of this work. This study was supported by FAPESP (São Paulo Research Foundation) through a scholarship awarded to the author Lucas Martins Morello, under grant number 2024/08607-6.

References

[1] Z.-a. Zheng, Z. Ye, and X. Zheng, "Intelligent vehicle lateral control strategy research based on feedforward+ predictive lqr algorithm with ga optimisation and pid compensation," *Scientific Reports*, vol. 14, no. 1, p. 22317, 2024.

[2] H. Jain and P. Babel, "A comprehensive survey of pid and pure pursuit control algorithms for autonomous vehicle navigation," 2024. [Online]. Available: https://arxiv.org/abs/2409.09848

[3] M. Rasib, M. A. Butt, S. Khalid, S. Abid, F. Raiz, S. Jabbar, and K. Han, "Are self-driving vehicles ready to launch? an insight into steering control in autonomous self-driving vehicles," *Mathematical Problems in Engineering*, vol. 2021, no. 1, p. 6639169, 2021. [Online]. Available: https://onlinelibrary.wiley.com/doi/abs/10.1155/2021/6639169

[4] J. M. Snider *et al.*, "Automatic steering methods for autonomous automobile path tracking," *Robotics Institute, Pittsburgh, PA, Tech. Rep. CMU-RITR-09-08*, 2009.

[5] C. Yang and J. Liu, "Trajectory tracking control of intelligent driving vehicles based on mpc and fuzzy pid," *Mathematical Problems in Engineering*, vol. 2023, no. 1, p. 2464254, 2023. [Online]. Available: https://onlinelibrary.wiley.com/doi/abs/10.1155/2023/2464254

[6] D. Mohanraj, R. Aruldavid, R. Verma, K. Sathiyasekar, A. B. Barnawi, B. Chokkalingam, and L. Mihet-Popa, "A review of bldc motor: state of art, advanced control techniques, and applications," *Ieee Access*, vol. 10, pp. 54 833–54 869, 2022.

[7] M. H. Rashid, "Eletrônica de potência: dispositivos, circuitos e aplicações," *Tradução de L. Abramowicz*, vol. 48, p. 48, 2014.

[8] T. Gillespie, *Fundamentals of vehicle dynamics*. SAE international, 2021.

[9] J. A. Reyes-Avendaño, L. I. Farfan-Cabrera, J. de Dios Calderon-Nájera, and H. G. González-Hernández, "Development of a simplified automated guided electric vehicle for testing and teaching automotive systems and navigation algorithms," *International Journal on Interactive Design and Manufacturing (IJIDeM)*, vol. 16, no. 4, pp. 1761–1777, 2022.